

University of Dundee

## Mechanical performance of statically loaded flat face epoxy bonded concrete joints

Newlands, Moray; Khosravi, Noushin; Jones, Roderick; Chernin, Leon

*Published in:*  
Materials and Structures

*DOI:*  
[10.1617/s11527-018-1175-2](https://doi.org/10.1617/s11527-018-1175-2)

*Publication date:*  
2018

*Licence:*  
CC BY

*Document Version*  
Publisher's PDF, also known as Version of record

[Link to publication in Discovery Research Portal](#)

*Citation for published version (APA):*  
Newlands, M., Khosravi, N., Jones, R., & Chernin, L. (2018). Mechanical performance of statically loaded flat face epoxy bonded concrete joints. *Materials and Structures*, 51(2), 1-14. [49]. <https://doi.org/10.1617/s11527-018-1175-2>

### General rights

Copyright and moral rights for the publications made accessible in Discovery Research Portal are retained by the authors and/or other copyright owners and it is a condition of accessing publications that users recognise and abide by the legal requirements associated with these rights.

- Users may download and print one copy of any publication from Discovery Research Portal for the purpose of private study or research.
- You may not further distribute the material or use it for any profit-making activity or commercial gain.
- You may freely distribute the URL identifying the publication in the public portal.

### Take down policy

If you believe that this document breaches copyright please contact us providing details, and we will remove access to the work immediately and investigate your claim.

# Mechanical performance of statically loaded flat face epoxy bonded concrete joints

Moray Newlands  · Noushin Khosravi  · Roderick Jones  · Leon Chernin 

Received: 24 March 2017 / Accepted: 12 March 2018  
© The Author(s) 2018

**Abstract** One of the main challenges in the offshore renewable energy industry is the reduction in the levelised cost of energy of wind, wave and tidal devices. The use of concrete as the primary construction material in such devices presents a low unit cost, high marine durability alternative to steel, however, to maximise material efficiency factors such as mix constituent design, structural detailing and manufacturing processes have to take into account the specific conditions of the marine environment. Pre-cast segmental construction can be considered as one of the fastest and cheapest construction options. However the challenges regarding performance of epoxy bonded concrete in marine environment should be taken into account. This paper presents the results of an experimental programme on the performance of shear and tensile capacity of flat face concrete joints, focussing on the effect of substrate surface preparation, joint thickness, properties of epoxy resins, exposure to seawater and presence of joint defects on the ultimate failure load. The ultrasonic pulse velocity (UPV) method for detection of defects in the adhesive layer was examined and digital image correlation is used to observe the surface strain flow through the joint. The results indicate that the epoxy joints behave monolithically and remain undamaged

under different types of static loading. The joints do not significantly interrupt the flow of strain but can locally affect the distribution of strain (and thus stiffness and stresses) in a structure. An increase in the density of the epoxy (and the filler content) leads to the increase in the joint strength and thicker joints are less affected by small defects in the bonding layer. The majority of tested specimens failed by cracking of concrete rather than by debonding of the joint, whilst compressive stresses acting on the joint can help to augment its shear strength. Sandblasting of bonded surfaces can improve performance of joints, whereas UPV testing may be used for quality control of epoxy-bonded joints.

**Keywords** Marine concrete · Flat face joints · Surface preparation · Epoxy bonding · Shear testing · Mechanical performance

## 1 Introduction

The use of concrete for offshore construction is well documented and can offer a cost-effective alternative to steel as the primary structural material in wave and tidal energy devices and floating wind turbines [1]. There are many performance criteria that will govern the design of these structures including materials considerations, durability, evaluation of dynamic

---

M. Newlands (✉) · N. Khosravi · R. Jones · L. Chernin  
School of Science and Engineering, University of Dundee,  
Dundee DD1 4HN, Scotland  
e-mail: m.d.z.newlands@dundee.ac.uk

loading, design approaches and certification requirements, manufacturing methods, deployment, operation and maintenance [2].

Renewable energy devices such as wave energy convertors have precise buoyancy requirements and will be affected by construction methodologies, defects and tolerances. Precast segmental construction is a proven method to achieve construction tolerances, however, this requires the use of bonded concrete joints. Resin-based bonding materials have been used in civil engineering applications such as segmental bridge construction [3] and for repair and strengthening of the concrete with externally bonded steel or fibre plates [4]. However, there is little precedent of epoxy bonded concrete in the marine environment.

Flat-faced joints offer easier, more rapid and lower cost construction compared to shear key joints. Earlier works on post-tensioned dry and epoxy bonded flat-faced joints and joints with single and multiple keys highlighted that, while all types of epoxy joints behaved monolithically and had similar strength, the presence of keys was important only in dry joints [5, 6]. Rombach [7] also conducted an experimental study on post-tensioned jointed system, the results showed that epoxy joints are much more brittle, although stronger. Turmo et al. [8] used hooked end steel fibre reinforced concrete and tested dry shear key joints under service and ultimate load. The results revealed that steel fibre reinforcement does not increase shear capacity of bonded concrete and high local shear or flexure stresses in the keys can cause various range of cracking of keys.

Assessing bond strength of fresh concrete overlays bonded to hardened concrete has shown that the quality of the bond is linked to the surface roughness [9–11]. Therefore, the use of various surface preparation techniques in an attempt to improve the bond strength of concrete overlays is common throughout the construction industry, but as bonding agents are introduced, the relationship between surface roughness and bond strength is unclear. Garbacz et al. [10], Júlio et al. [12] and Santos et al. [13] concluded that the application of a bond coat unified the adhesion level, negating the influence of surface roughness especially in cases of bonding hardened concrete to hardened concrete.

The influence of the bonding agent is also of interest in relation to the differential stiffness between the bonding agent and the concrete layers; and the

influence of thickness on the behavior of the joint and ultimate strength. Regarding the thickness of the adhesive layer, existing data is very scarce. Studies of Derewonko et al. [14], Frigione et al. [15] and Da Silva et al. [16] showed sensitivity of bond strength to thickness of the adhesive in thin joints (0.5–2 mm), which is not normally the case with structural adhesives in civil engineering applications.

Moreover, Abu-Tair et al. [17] and [18], Bonaldo et al. [19], Santos and Julio [11, 20] and [13], Tayeh et al. [21] and many others with all sorts of splitting, pull off and slant shear tests showed that bond strength is very much dependant on the test method and the results can be very scattered. The failure modes can also change from adhesive failure to cohesive or mixed failure.

At present, little work has been carried out on bonded joints subjected to cycles of seawater wetting and drying. Knox and Cowling [22] and Broughton and Mera [23] studied the effect of temperature and humidity on thin bonded metal joints and reported that exposure to extremes can cause plasticization of adhesives and a strength reduction of the resins. The effect of seawater salt solutions on the mechanical behaviour of resin-bonded concrete surfaces has not been investigated.

In this present study, some of the important variables mentioned above including the effect of epoxy type and joint thickness on structural capacity of flat-face concrete joints are examined and some guidance on the suitability of flat-face joints as a low cost method in marine construction provided.

## 2 Structural mechanics test programme

The main aim of the test programme was to determine the influence of substrate preparation, joint thickness, epoxy type and workmanship on the shear and tensile performance of flat-faced epoxy joints. A range of substrate preparations were examined (no preparation, sand blasting and wire brushing) based on typical methods used in concrete surface preparations for joining concrete sections [10, 12, 13]. In addition, joint thicknesses of 2, 3 and 4 mm were examined, as these are sizes typically used in industry [24] and shear and tensile tests were undertaken using a combination of standard and non-standard methods (where standard methods do not take jointed concrete into



consideration). To examine the effect of workmanship, defects were introduced to the joints (10 and 50% surface area defects) and ultrasonic pulse velocity (UPV) used to assess whether the defects were measurable prior to testing. Six commercially available epoxies (epoxies A–F) were chosen based on their popularity amongst industry and the fact that they had range of tensile, shear and bond characteristics. An additional study examining the influence of epoxy exposure to simulated seawater was also undertaken. Digital image correlation (DIC) was also used on selected specimens to examine surface strain across the flat-faced joints during the test procedures.

Given the number of variables it was not possible test all combinations. Table 1 gives details of those variables selected with the main basis being that all test methods could be compared across all epoxy types at one joint thickness (typically 3 mm). The influence of joint thickness was confined to epoxy A, B and C (given their variable properties) and seawater and DIC studies focussed on epoxy B with a joint thickness of 3 mm.

Table 1 also shows the number of specimens tested in each series, for example, 3NP, 3SB, 3WB means that 3 untreated (NP), 3 sand blasted (SB) and 3 wire brushed (WB) specimens were tested. Where possible, at least 3 specimens were tested within the main series. Six specimens of each joint thickness with an induced 10 and 50% surface area defect were also examined using the bi-surface shear test and prior to testing, these specimens were inspected using UPV.

This study used the standard test method, BS EN 12615 for slant shear [25], which results in a relatively uniform stress distribution at the joint and is generally sensitive to a range of parameters [12, 17, 20], and for comparison, a bi-surface shear test devised by Momayez et al. [26] developed for assessing bonded joint behaviour. In addition, the split cylinder test (BS EN 12390-6) [27] and flexural strength test (BS EN 12390-5) [28] were modified for bonded specimens to determine the mechanical performances of the flat-faced joints. UPV was tested to BS EN 12504-9 [29].

## 2.1 Jointed section shear capacity test methods

The slant shear method, BS EN 12615 [25], comprises a  $400 \times 100 \times 100$  mm concrete prism with an epoxy-bonded joint inclined at  $30^\circ$  to the main axis of the prism, subjected to axial compression (joint area

is  $100 \times 200$  mm). The test standard states that joint bond strength is calculated by dividing the failure load by the area of the bonded surface, however, forces at the joint includes the shear ( $S$ ) and compressive ( $C$ ) forces which are the components of the axial compression force ( $P$ ) applied to the concrete prism. In the current study,  $S$  and  $C$  were determined by:

$$S = P \cos(30^\circ) = 0.87P \quad (1a)$$

$$C = P \sin(30^\circ) = 0.50P \quad (1b)$$

It should be noted that  $C$  is directly proportional to  $S$ , i.e.,  $C = S \tan(30^\circ) = 0.577 S$  and the ultimate shear force divided by the joint area was used to enable a direct comparison with the bi-surface shear test.

The bi-surface shear test [26] was also used to evaluate the joint bond strength under shear stress. Two similar experimental setups shown in Fig. 1 were implemented to examine the effectiveness of this testing method. Both versions comprise a 150 mm concrete cube specimen with a flat face joint located at 50 mm from one of cube sides. In Setup 1 (Fig. 1a) the specimen is positioned on two 50 mm wide steel plates on rollers placed along cube edges parallel to the joint, while the load is applied through a third roller positioned on a 50 mm wide steel plate at the top face of the larger concrete segment parallel to the joint. In Setup 2 (Fig. 1b), the specimen is placed on two 30 mm wide steel plates on rollers, while the load is applied through a 50 mm wide roller placed on the top of the larger concrete segment, 30 mm from the joint. In both cases, the joint is in the main subjected to shear stress, since bending stress is negligible due to the lever arm being too small. The presence of the joint eliminates the symmetry in applied loads and thus influences the shear force acting on the joint. To eliminate this geometrical effect, the shear force has been calculated for specimens with different joint thickness as shown in Table 2. In the experimental programme, Setup 1 was used for specimens bonded by the epoxy A, while Setup 2 for specimens bonded by epoxies B–F (the characteristics of the epoxies are detailed in Table 4). Since the differences between test setups lay mainly in the localised effects around different loading and supporting arrangements (which have negligible effect on the shear stress in the joint), the results obtained from both setups can be compared. In the bi-surface shear tests, the shear strength of the joint was evaluated as the peak shear force calculated

**Table 1** Experimental programme

Epoxy code <sup>a</sup>	Test method	Nominal joint thickness			Sea water tidal tank (90 day exposure) 3 mm	DIC <sup>d</sup> 3 mm
		2 mm	3 mm	4 mm		
A	Slant shear	3NP	3NP	3NP	–	–
		3SB	3SB	3SB		
		3WB	3WB	3WB		
	Bi-surface shear	3NP	3NP	3NP	–	–
	Bi-surface shear, defect <sup>b</sup> , UPV <sup>c</sup>	3NP (10%), 3NP (50%)	3NP (10%), 3NP (50%)	3NP (10%), 3NP (50%)	–	–
	Split cylinder	6NP	6NP	6NP	–	–
		3SB	3SB	2SB		
		3WB	3WB	3WB		
	Flexure	3NP	3NP	3NP	–	–
		3SB	3SB	3SB		
		3WB	3WB	3WB		
B	Slant shear	–	1NP	1NP	1NP	1SB
			4SB	6SB	4SB	
	Bi-surface shear	–	1NP, 5SB	1NP		
				6SB		
	Split cylinder	–	2SB	–	–	
C	Flexure	–	3SB	–	–	
	Slant shear	–	3SB	3SB	–	–
D	Bi-surface shear	–	3SB	3SB	–	
	Slant shear	–	3SB	–	–	–
E	Bi-surface shear	–	4SB	–	–	
	Slant shear	–	2SB	–	–	
F	Bi-surface shear	–	2SB	–	–	
	Slant shear	–	2SB	–	–	–

–, not tested; NP, no surface preparation; SB, sand blast surface preparation; WB, wire brush surface preparation

<sup>a</sup>Epoxy codes detailed in Table 4

<sup>b</sup>Defect (in %) induced by reducing epoxy coverage on joint

<sup>c</sup>Ultrasonic pulse velocity

<sup>d</sup>Digital image correlation

in accordance with Table 2 divided by the area of the bonded surface.

### 2.1.1 Effect of induced defects on joint shear capacity

Specimens were also designed with two induced defects, namely, (1) 10% defect–90% epoxy coverage, and (2) 50% defect–50% epoxy coverage, with a control specimen having no defect (100% epoxy coverage of the joint). Defects were created by covering part of the surface of the joint with a plastic card to prevent epoxy coverage. This technique

enabled to control the location and the area of the defect during specimen preparation. UPV measurements were conducted across and through the joint plain, to determine UPV suitability in detecting the defects.

### 2.1.2 Effect of artificial seawater exposure on shear capacity

Test specimens were also exposed to 24 h wetting/drying cycles (wetting for 6 h and fan assisted drying for 18 h) in artificial seawater salt solution (3.5% NaCl



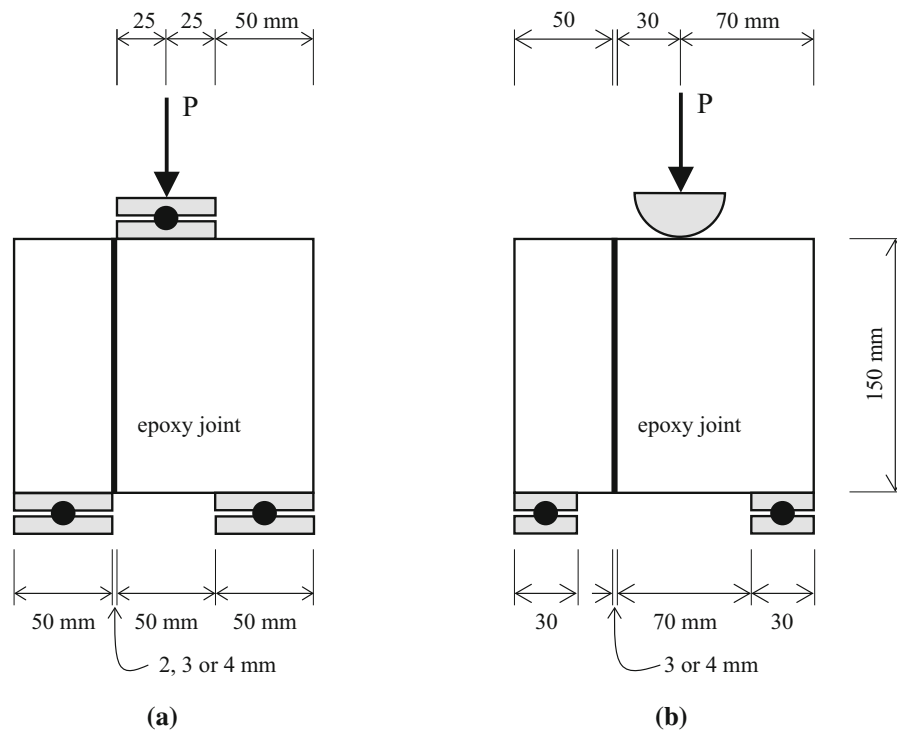


**Fig. 1** Bi-surface shear test: **a** Setup 1 and **b** Setup 2

**Table 2** Shear force in the joint in the bi-surface shear test

Joint thickness (mm)	Shear force in joint	
	Setup 1 (epoxy A)	Setup 2 (epoxy B–F)
2	0.48P	–
3	0.47P	0.43P
4	0.46P	0.42P

solution at  $20 \pm 2$  °C) for 90 days prior to shear testing.

## 2.2 Jointed section tensile capacity test methods

A modified version of the split cylinder test, BS EN 12390-6 [27] was used to determine the indirect tensile capacity of joints. Cylindrical specimens (100 mm diameter and 300 mm in length) were manufactured with an epoxy-bonded joint dividing the cylinder into two equal parts along its length. The compressive load was applied on the joint and, as a result, the joint was in the state of compression in its plane and tension out of the plane.

A modified version of the flexural four-point bending test, BS EN 12390-5 [28] was used to

determine the influence of joints on the flexural capacity of concrete. The supporting and loading conditions of the beam were fully symmetrical and in this study, an epoxy-bonded joint was introduced at the midpoint of the beam. As a result, the joint was subjected to tensile stresses in its lower half.

## 2.3 Strain monitoring of jointed specimens in shear and tensile testing

The evolution of strain fields and hence stiffness distribution on the surface of specimens during shear and tensile testing was monitored using Digital Image Correlation (DIC). DIC is an optical method based on the use of two Photron SA-1 high speed video cameras able to capture up to 5400 frames per second at 1

megapixel resolution and software VIC-3D [30]. The examined specimen surface was coloured white with a reference grid of black dots and two cameras were positioned to record the specimen surface from different angles. Reference photographs were taken before testing began and the displacements of the reference dots were recorded during the test by the cameras with a pre-set speed. The surface strain fields were calculated for each photograph, with strain measurements to nearest micro-strain ( $\mu\text{m}/\text{m}$ ).

## 2.4 Materials used

The concrete mix used in the experimental programme was a 50% GGBS concrete (C III/A) conforming to BS 8500-2 [31] which is typical of marine and coastal structures in Europe (Table 3). All mixing procedures conformed to BS 1881-125 [32].

Specimens were standard water cured ( $20 \pm 2^\circ\text{C}$ ) for 28 days. The slant shear and split cylinder test specimens were cast as two halves. The bi-surface and flexure specimens were cast whole and then cut in two using a diamond saw at 28 days.

The study investigated six epoxies to determine the sensitivity of material characteristics on the mechanical properties of the joint. Table 4 presents general and mechanical characteristics as supplied by the manufacturers.

### 2.4.1 Joint substrate preparation

Joint substrate surfaces were prepared (either mechanically sand blasted until aggregates were visible, or wire brushed by hand for 30 s prior to application of epoxy) to determine the influence of surface roughness on the bond and joint mechanical properties.

### 2.4.2 Application of epoxy to substrate

Application of the epoxy to the substrate was carried out by hand. Surface substrates were conditioned ( $20 \pm 2^\circ\text{C}$ ,  $55 \pm 5\%$  rh) for 24 h prior to application. Joint thickness on all specimens was controlled by means of plastic tiling spacers and jointed specimens were kept in laboratory conditions for 3 days after epoxy application to allow for curing of the epoxy.

## 3 Performance of jointed concrete sections

### 3.1 Characterisation of failure modes

In all test methods, failure of specimens was characterised in one of three ways. Failure either occurred:

1. In the concrete near the joint (cohesive failure),
2. In the epoxy bonding material (adhesive failure) or
3. Through a combination of failure of the concrete and the epoxy bonding material (mixed failure).

### 3.2 Shear capacity of jointed concrete sections

#### 3.2.1 Modes of failure

Cohesive failure was the dominant failure mode occurring in 51% of all shear tests with adhesive failure occurring in 28% of tests and the remainder being mixed mode failure. The majority of specimens with epoxy A failed by adhesive failure in the slant shear test, and cohesive failure in the bi-surface shear test. This aligns with the low compressive strength and

**Table 3** Test concrete mix proportions and selected properties

Constituent proportions (kg/m <sup>3</sup> )					SP <sup>b</sup> (%)	Selected properties			
CEM I 52.5 N	GGBS	Water	Aggregates <sup>a</sup>			w/c ratio	Plastic density (kg/m <sup>3</sup> )	Slump (mm)	f <sub>c</sub> , 28 days (MPa)
			Fine 0/5	Coarse 5/20					
225	225	170	680	1090	0.4	0.38	2390	100	60

<sup>a</sup>Coarse aggregate and granite fine aggregate glacial sand (1% water absorption)

<sup>b</sup>Superplasticizer, % of total cementitious material by weight



**Table 4** Epoxy characteristics based on manufacturer data sheet

General characteristics									
Epoxy code	Recommended temperature range (°C)	Thermal expansion coefficient (1/°C)	Shrinkage (%)	TG <sup>a</sup> (°C)	Density (kg/l)	Resin content (%)	Hardener content (%)	Filler content (%)	Mix Ratio <sup>b</sup> (resin: hardener + filler)
A	+ 10 to + 30	$9.3 \times 10^{-5}$	0	+ 49	1.35	50	50		1:1
B	+ 8 to + 35	$2.5 \times 10^{-5}$	0.04	+ 62	1.65	25	75		1:3
C	Min 5	nd	nd	41.5	1.02	50	50		1:1
D	Min 5	nd	nd	nd	1.85	19	4	77	nd
E	+ 5 to + 45	nd	nd	nd	1.60	23	7	70	nd
F	nd	nd	nd	nd	nd	63	37	nd	nd
Mechanical characteristics									
Epoxy code	Strength characteristics (MPa)					Moduli characteristics (GPa)			Tensile elongation (%)
	Compressive	Flexural	Shear	Tensile	Bond <sup>c</sup>	$E_{\text{compressive}}$	$E_{\text{tensile}}$	$G_{\text{shear}}$	
A	50	nd	20	10–15	> 5	nd	nd	nd	nd
B	65 – 75	nd	13–16	21–24	> 4	9.6	11.2	1.5	nd
C	56.7	60.8	nd	32.7	nd	nd	2.58	nd	3.3
D	80	21	nd	13.2	3.8	nd	nd	nd	nd
E	65	34	nd	14	5.9	nd	nd	nd	nd
F	nd	65	nd	41	nd	nd	nd	nd	nd

nd no data

<sup>a</sup>Glass transition temperature

<sup>b</sup>Mix ratio by mass

<sup>c</sup>Based on substrate failure

high shear strength of the epoxy A. The dominance of the cohesive mode of failure in specimens with epoxies B, C, D and E tested with the slant shear method can be attributed to the higher compressive strength of these epoxies as the slant shear test subjects specimens to both shear and compression and will thus be influenced by both the shear and compressive properties of the epoxies tested.

All slant shear test specimens bonded by epoxy F failed with the adhesive mode. This indicates that the shear strength of epoxy F is lower than that of the concrete used in the tests. Although the tensile strength is relatively high (65 MPa) the resin content is also high (63%) and no filler is present which will also influence the shear capacity of the epoxy.

In the slant shear tests, increasing the joint thickness resulted in an increase in adhesive failures. This was seen rate of 11% increase per 1 mm joint

thickness for the epoxy A and 13% per 1 mm for the epoxy B with the number continuing to increasing with joint thickness. It should also be noted that failure mode was not influenced by substrate preparation but indicated that as the joint thickness increased, the stress pattern over the joint may be changing with stresses moving from the concrete into the epoxy as the joint thickness increased. This effect was not seen in the bi-surface shear data with the pattern of failure modes being less consistent. Exposure of specimens in the tidal tank resulted in a change in dominance of failure mode to cohesive failure in the bi-surface shear test.

### 3.2.2 Comparison of calculated shear strength

Figure 2 compares the calculated shear strength of jointed specimens, with shear from the slant shear test



based on Eq. 1a. The slant shear test yielded higher joint shear strengths than the bi-surface shear test regardless of surface preparation, type of epoxy resin and thickness of joint. This increase highlighted the influence of compressive action in the slant shear test which could lead to increase interlocking and friction forces at the concrete/epoxy interface compared to bi-surface shear tests which are assumed to be acting purely in shear. It can be inferred from Fig. 2 that the compressive stresses associated with the slant shear test, comprising about 58% of the shear stresses, lead to increased shear strengths by approximately 3–4 times that of the bi-surface shear test method.

All joints had shear strengths which were higher than the manufacturer bond strength data (Table 4), however, specimens that failed in adhesive mode had shear strengths smaller than that of the bulk epoxy. Epoxy F showed the lowest joint shear strength and failed in the adhesive mode (see Fig. 2). Therefore, this epoxy was deemed to be unsuitable for the segmental construction of floating marine concrete structures and was excluded in the rest of the experimental programme. The other epoxies performed much better in the shear tests.

The influence of substrate preparation was less clear with control specimens (no substrate preparation) exhibiting marginally higher strengths in 2 and 4 mm joints. In most slant shear tests, the surface

preparation had limited influence on the shear strength, however, in all cases, wire brushing preparation showed lower shear strengths and was thus deemed unsuitable as a surface preparation method. Sandblasting was chosen as the comparative method for the influence of epoxy type as it is common practice in industry.

### 3.2.3 Effect of artificial seawater cyclic wetting and drying on shear capacity

Table 5 compares the shear strength of specimens before and after 90 days' exposure to artificial seawater. Control specimens (no substrate preparation) showed a small reduction in shear strength with both slant shear (12%) and bi-surface shear (3%). Preliminary results show that specimens with sandblasted substrate preparation have increased shear strength indicating that in the long term, surface preparation may be an important factor. However, the tests were executed on a very limited number of specimens and further research is necessary to validate this conclusion. An examination of failure modes also showed a shift from cohesive to adhesive failure, however, this may have been influenced by the extended curing period of the concrete due to the length of the test method.

**Fig. 2** Calculated shear strength from the slant (SS) and bi-surface (BS) shear tests

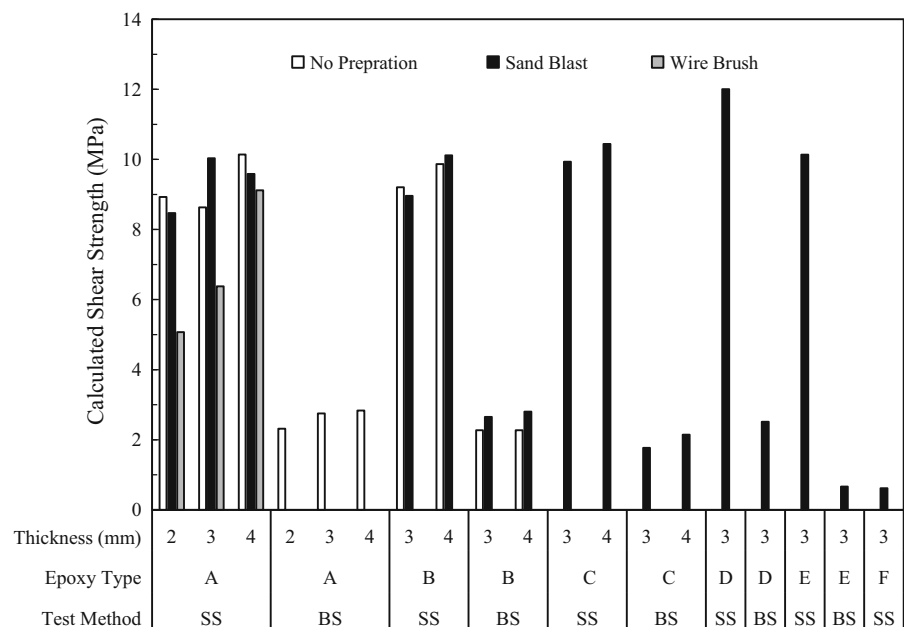


**Table 5** Effect of simulated seawater exposure on shear strength

Type of exposure	Shear strength (MPa)			
	Slant shear test		Bi-surface shear test	
	NP <sup>a</sup>	SB <sup>b</sup>	NP <sup>a</sup>	SB <sup>b</sup>
No tidal exposure	10.58	10.30	2.29	2.65
90 days of tidal exposure	9.35	14.48	2.21	3.15

<sup>a</sup>No surface preparation<sup>b</sup>Sand blast surface preparation

### 3.2.4 Surface shear strain

Figure 3 depicts the distributions of the surface shear strain ( $\gamma_{xy}$ ) just prior to the point of failure in both the slant and bi-surface shear tests. Both tests showed cohesive failure of the specimens. The approximate positions of the joints are shown in the Fig. 3 by the dashed line.

As can be seen in Fig. 3a, the presence of the inclined joint affected the shear strain field across the specimen. The distribution of shear strain along the joint was not uniform. Two zones of high shear strain (reaching  $\gamma_{xy} = -0.0063$  in Fig. 3a) developed at both ends of the joint at early stages of the slant shear test and remained there throughout the test until failure. This possibly occurred due to localised

variations of stiffness in the concrete introduced by the joint. Strain concentrations at the top and bottom ends of the specimen developed due to the influence of the boundary conditions and can be disregarded. The shear strain in the areas between the high strain zones gradually decreased to zero. At the stage of the tests shown in Fig. 3a, the field of the shear strain across the joint was uninterrupted by any discontinuities and the specimen still behaved monolithically.

In the bi-surface shear test, two high shear strain zones developed at the internal end of the loading plate supporting the smaller concrete segment and at the top roller. These strain concentrations grew with the increase in the load until they merged as shown in Fig. 3b creating a high shear strain band passing along and across the joint. At the stage of the tests shown in

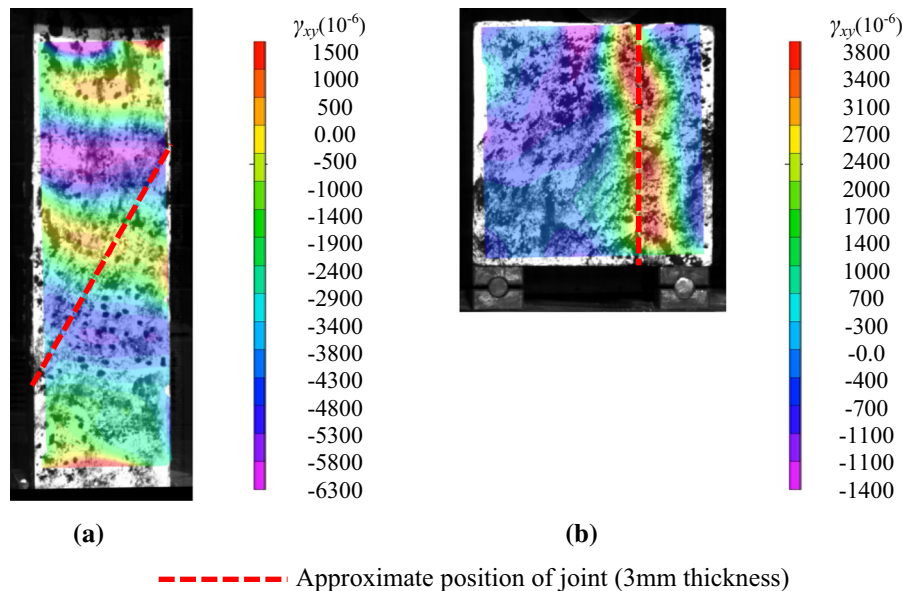
**Fig. 3** Surface shear strain  $\gamma_{xy}$  distribution for **a** the slant and **b** bi-surface shear tests using epoxy B and a joint thickness of 3 mm

Fig. 3b, the shear strain around the joint was continuous with the maximum reaching  $\gamma_{xy} = 0.0038$  and the specimen behaved monolithically. The distribution of shear strain in the joint was close to uniform by the end of the test and as a result, the bi-surface shear test can be a very efficient method for evaluation of the shear strength of joints. It should however be emphasized that Fig. 3 shows the field of the surface shear strain in both slant shear and bi-surface shear tests and may be not indicative of the strain distribution in depth of the joint which can be different due to boundary effects or presence of defects.

### 3.2.5 Effect of induced defects on shear capacity

The influence of induced defects on shear strength and the average UPV value through and across the joint is shown in Table 6. In general, with the same joint thickness maintained, the induced defects lead to a loss of shear strength however the influence was reduced with thicker joints indicating that thicker joints may suitable for offsetting likely workmanship issues resulting in relatively small defects. Table 6 also shows that the UPV method was sensitive to the presence of defects and there was a reasonable correlation between the presence of the defect and the UPV readings.

## 3.3 Tensile capacity of jointed concrete sections

### 3.3.1 Modes of failure

The cohesive mode of failure was the most common whilst adhesive mode was only observed in the flexural test. All specimens bonded by epoxy B failed in the cohesive mode regardless of the test method while in the split cylinder test for epoxy A 17, 50 and 18% of joints with 2, 3 and 4 mm thickness, respectively, failed in the mixed mode and there was no case of adhesive failure. Regarding flexure test with epoxy

A, 22 and 33% of mixed failure for 2 mm and 4 mm joints, and 22, 11 and 22% of adhesive failure for 2, 3 and 4 mm joints correspondingly was observed.

### 3.3.2 Tensile strength of jointed sections

Figure 4 shows the average tensile strength of jointed specimens along with the strength of control non-jointed specimens obtained using the split cylinder and flexural tests. In all but one case with epoxy A, the jointed specimens had a lower strength compared to the control, with an average reduction of around 26% for the split cylinder test and 6% for the flexural strength. The flexural test on jointed specimens yielded an average tensile strength of around twice that obtained with the split cylinder test using epoxy A however specimens bonded by epoxy B exhibited the opposite behaviour with the flexural test giving a lower tensile strength.

CEB-FIP Model Code 2010 [33] states the mean value of the characteristic tensile strength of a 60 MPa concrete is  $f_{ctm} = 4.4$  MPa, with lower and upper bound values, (5 and 95% fractiles) equal to 3.1 MPa ( $f_{ctk,min}$ ) and 5.7 MPa ( $f_{ctk,max}$ ), respectively. Only the split cylinder test specimens bonded by epoxy A showed the tensile strengths that were lower than the Model Code values.

Figure 4 shows that flexural tests lead to larger values of tensile strength than the split cylinder tests. This phenomenon is the result of inherent differences in the testing techniques. According to Jackson and Dhir [34] the ratio between the tensile strengths obtained in the flexural and direct tensile tests is expected to be around 1.56. Given that the tensile strength obtained from the direct tensile test should be about 5–12% less than that from the split cylinder test [35], the ratio between the tensile strengths obtained from the flexural and split cylinder tests should be in the range of 1.39–1.48. The tests on the control non-

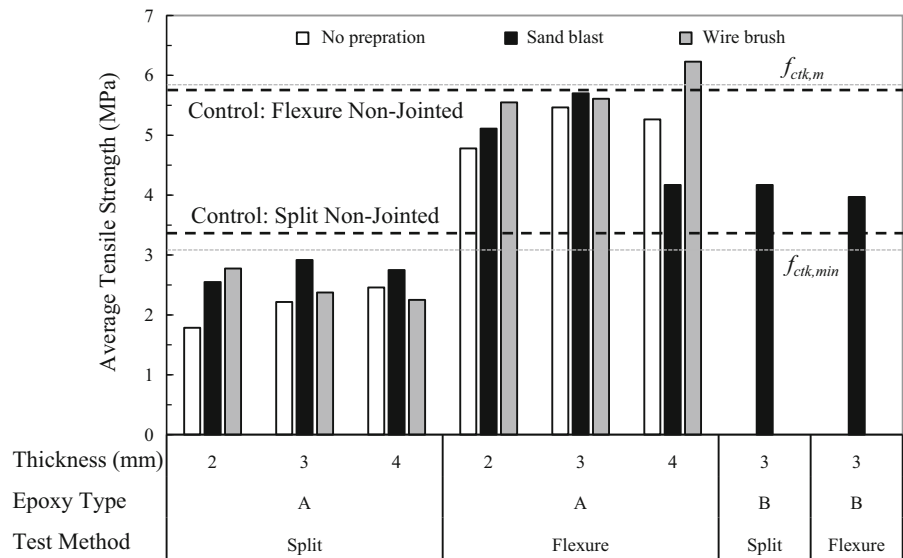
**Table 6** Effect of induced defect on shear strength and UPV reading

	Control (no defect)			10% defect			50% defect		
Joint thickness (mm)	2	3	4	2	3	4	2	3	4
Shear strength <sup>a</sup> (MPa)	2.30	2.76	2.88	1.95	2.51	2.84	1.07	1.73	2.19
Loss of shear strength (%)	–	–	–	15.3	9.1	1.6	53.5	37.2	24.2
Mean UPV <sub>H</sub> (km/s)	4.77	4.75	4.70	4.68	4.63	4.56	4.07	4.17	3.97
Mean UPV <sub>V</sub> (km/s)	4.72	4.58	4.68	4.63	4.54	4.58	4.37	4.39	4.42

<sup>a</sup>Measured using bi-surface test method only



**Fig. 4** Ultimate tensile stress considering various epoxies, surface preparation and joint thickness



jointed specimens yield the ratio equals 1.46 (see Fig. 4) which is within the calculated range.

The control specimens showed higher strength than the jointed specimens except in the split cylinder test with the epoxy B and in the flexural test with the 3 mm sandblasted joint and the 4 mm wire brushed joint both bonded by the epoxy A. This phenomenon and the fact that most of the specimens failed with the cohesive mode can be the result of the stress concentrations in the concrete introduced by the presence of the joint.

The specimens bonded by epoxy B showed higher tensile strength in the split cylinder tests compared to the epoxy A as expected since epoxy B has higher tensile strength (see Fig. 4). However, the tensile tests resulted in a sufficiently smaller tensile strength for epoxy B.

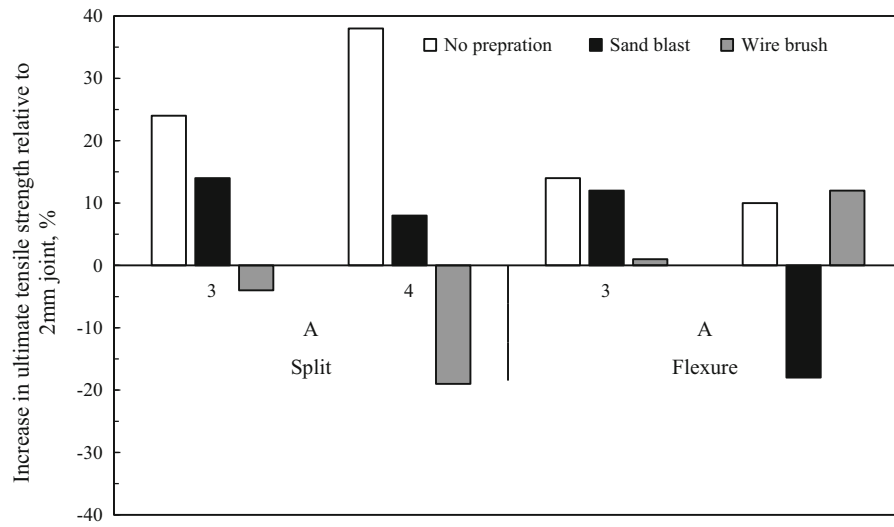
The experimental data in Fig. 5 shows that specimens with no substrate preparation were more sensitive to joint thickness with a joint increase from 2 to 4 mm leading to a 40% increase in strength in the split cylinder test. The effect of the increase in thickness on the sandblasted joints was much smaller, while wire brushing exhibited negative influence. In the flexural test, the increase in the joint thickness generally led to the increase in its tensile strength except for the 4 mm thick sandblasted joint. In most cases, the increase in the surface roughness by sandblasting or wire brushing was beneficial for the tensile strength of the joint. Surface preparation had

bigger effect on thinner joints especially in the split cylinder test.

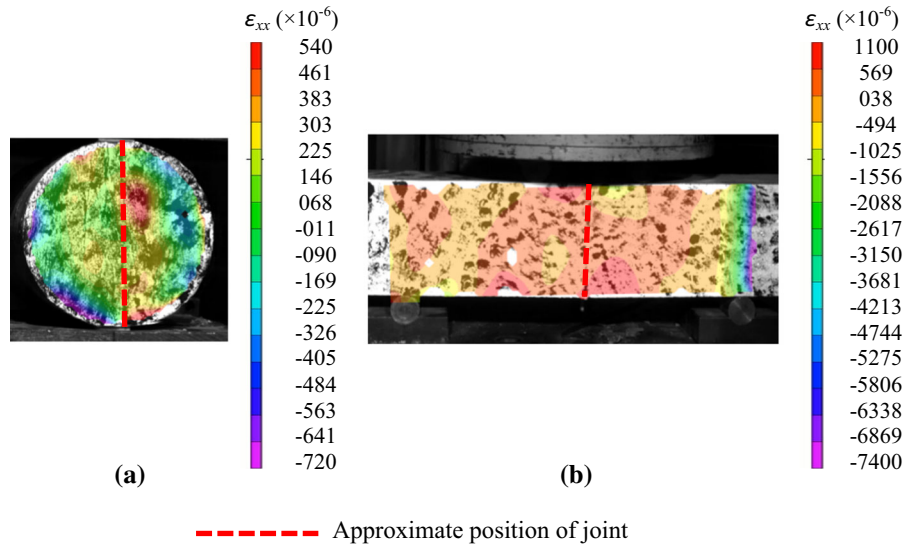
### 3.3.3 Surface tensile strain

Figure 6 shows the distribution of the surface horizontal strain ( $\epsilon_{xx}$ ) obtained using the DIC method in the split cylinder and modified flexural tests close to specimen failure.  $\epsilon_{xx}$  was analysed as it provided direct information about the flow of the tensile strain across at the joint. The position of the joint is emphasised in Fig. 6 by the dashed line.

During the split cylinder test, a band of high tensile strain developed in the middle of the cylinder. This strain band, visible in Fig. 6a, started at the cylinder top from the left of the joint and at the bottom from its right and then connected at the middle. The band was wider in the left half of the cylinder. The presence of the joint did not appear to interrupt the strain field during the test, although there was a zone of high strain concentration (reaching  $\epsilon_{xx} = 0.00054$  in Fig. 6a) to the right of the joint. The strain concentrations at the top and bottom of the cylinder were introduced by the boundary conditions and can be disregarded. The cylinder failed in the cohesive mode by splitting from the left of the joint. The crack originated at the strain concentration at the cylinder top and progressed downwards parallel to the joint. Full cylinder splitting followed by the joint debonding due to dynamic redistribution of stresses in the cylinder.



**Fig. 5** Comparative effect of joint thickness on joint tensile strength



**Fig. 6** Surface strain  $\varepsilon_{xx}$  distribution for **a** the split cylinder and **b** flexural tests, both tests with 3 mm sandblasted epoxy B joint

In the flexural test, a zone of high tensile strain (reaching  $\varepsilon_{xx} = 0.000569$  in Fig. 6b) developed to the right from the joint close to the bottom surfaces of the beam. The band of high strain values developed on the right of the beam should be ignored as it was most likely introduced by the influence of the support. The joint did not interrupt the flow of strain during testing and the specimen behaved as monolithic. The beam failed in the cohesive mode. The crack originated in the tensile zone of the beam at the strain concentration

on the right of the joint and progressed upwards throughout the beam depth from its bottom surface.

The cohesive failure observed in both tests can be explained by the fact that epoxy B was much stronger in tension ( $f_{tu} = 21\text{--}24$  MPa see Table 4) than the concrete ( $f_{ctk,max} = 5.7$  MPa according to CEB-FIP Model Code 2010 [33]).

## 4 Conclusions

The paper presents the results of a laboratory experimental programme investigating mechanical performance of flat face concrete joints bonded by epoxy resin under shear and tension.

Three standard modes of failure were observed, (1) cohesive, (2) adhesive and (3) mixed failure and across all tests, cohesive failure was most common, indicating that the performance of the epoxy bonding agents on the whole was suitable and that all jointed specimens behaved monolithically until failure. However, the failure mode and joint strength were sensitive to the thickness of the joint, the mechanical properties of the epoxy and concrete, presence of defects in the adhesive layer and exposure to simulated seawater. In general, an increase in joint thickness (from 2 to 4 mm) led to an increase in joint shear and tensile strength, however, this was sensitive to the concrete substrate preparation prior to the addition of epoxy. Sandblasting preparation had a positive influence, particularly on the tensile behaviour of joints whilst it also showed potential to enhance long-term shear strength at 90 days. The presence of the compressive stresses at the joint significantly augmented its shear strength. In the slant shear tests, the compressive stresses comprising about 58% of the shear stresses led to the increase of the joint shear strength by 3–4 times. The sensitivity of joint shear strength to defects was more evident in thinner joints and the UPV test method could detect such defects in thick joints and showed good correlation between its readings and defect size.

The DIC analysis showed that the presence of joints did not create discontinuities in the flow of strain in specimens, however, the joints could affect the uniformity of the strain fields. Cracks always initiated inside zones of strain concentration and propagated along bands of high strain. The bi-surface shear test was found to be a very efficient method for evaluation of joint shear strength due to a band of high shear strain developing along the joint, which led to a relatively uniform distribution of strain in the joint.

The work has shown that there is potential for using flat-faced joints in concrete structures however care must be taken with regards to achieving the required joint thickness as workmanship defects may have a larger influence on thinner joints. Further studies on the joint in marine environment is required and the research group is currently conducting testing on

effect of dynamic loading on bonded concrete and monitoring micro-crack growth in marine environment under cyclic loading.

**Acknowledgements** The authors would like to express their gratitude to Mr. Jon Benzie senior engineer at Quoceant Ltd. for his valuable input to this project, also acknowledge hard work and help of all the students at University of Dundee who conducted sample preparation and testing. Special thanks to all the epoxy manufacturers who supplied materials samples and the EPSRC Engineering Instrument Pool which supplied the DIC cameras and software.

**Open Access** This article is distributed under the terms of the Creative Commons Attribution 4.0 International License (<http://creativecommons.org/licenses/by/4.0/>), which permits unrestricted use, distribution, and reproduction in any medium, provided you give appropriate credit to the original author(s) and the source, provide a link to the Creative Commons license, and indicate if changes were made.

## References

1. Anderson C (2003) Pelamis WEC—main body structural design and materials selection. Department of Trade and Industry (DTI), Ocean Power Delivery Ltd., Scotland
2. ACI Committee 357 (2010) Report on floating and float-in concrete structures. American Concrete Institute, Farmington Hills
3. The Concrete Society (2010) Technical report 72: durable post-tensioned concrete structures. The Concrete Society, Camberley
4. Pellegrino C, Sena-Cruz J (2015) Design procedures for the use of composites in strengthening of reinforced concrete structures: state-of-the-art report of the RILEM technical committee 234-DUC, vol 19. Springer, New York
5. Koseki K, Breen JE (1983) Exploratory study of shear strength of joints for precast segmental bridges. Center for Transportation Research, The University of Texas at Austin, Austin
6. Saibabu S, Srinivas V, Sasmal S, Lakshmanan N, Iyer NR (2013) Performance evaluation of dry and epoxy jointed segmental prestressed box girders under monotonic and cyclic loading. *Constr Build Mater* 38:931–940
7. Rombach G (2002) Precast segmental box girder bridges with external prestressing-design and construction. INSA Rennes Technical University, Hamburg-Harburg
8. Turmo J, Ramos G, Aparicio AC (2006) Shear strength of dry joints of concrete panels with and without steel fibres: application to precast segmental bridges. *Eng Struct* 28(1):23–33
9. Santos PM, Júlio EN (2013) A state-of-the-art review on roughness quantification methods for concrete surfaces. *Constr Build Mater* 38:912–923
10. Garbacz A, Górka M, Courard L (2005) Effect of concrete surface treatment on adhesion in repair systems. *Mag Concr Res* 57(1):49–60



11. Santos PM, Julio EN (2007) Correlation between concrete-to-concrete bond strength and the roughness of the substrate surface. *Constr Build Mater* 21(8):1688–1695
12. Júlio E, Branco F, Silva V (2005) Concrete-to-concrete bond strength: influence of an epoxy-based bonding agent on a roughened substrate surface. *Mag Concr Res* 57(8):463–468
13. Santos DS, Santos PM, Dias-da-Costa D (2012) Effect of surface preparation and bonding agent on the concrete-to-concrete interface strength. *Constr Build Mater* 37:102–110
14. Derewonko A, Godzimirski J, Kosiuczenko K, Niezgoda T, Kiczko A (2008) Strength assessment of adhesive-bonded joints. *Comput Mater Sci* 43(1):157–164
15. Frigione M, Aiello M, Naddeo C (2006) Water effects on the bond strength of concrete/concrete adhesive joints. *Constr Build Mater* 20(10):957–970
16. Da Silva LF, Carbas R, Critchlow GW, Figueiredo M, Brown K (2009) Effect of material, geometry, surface treatment and environment on the shear strength of single lap joints. *Int J Adhes Adhes* 29(6):621–632
17. Abu-Tair A, Rigden S, Burley E (1996) Testing the bond between repair materials and concrete substrate. *ACI Mater J* 93(6):553–558
18. Abu-Tair A, Lavery D, Nadjai A, Rigden S, Ahmed T (2000) A new method for evaluating the surface roughness of concrete cut for repair or strengthening. *Constr Build Mater* 14(3):171–176
19. Bonaldo E, Barros JA, Lourenço PB (2005) Bond characterization between concrete substrate and repairing SFRC using pull-off testing. *Int J Adhes Adhes* 25(6):463–474
20. Santos PM, Júlio ENBS (2011) Factors affecting bond between new and old concrete. *ACI Mater J* 108(4):449–456
21. Tayeh BA, Bakar BA, Johari MM, Voo YL (2012) Mechanical and permeability properties of the interface between normal concrete substrate and ultra high performance fiber concrete overlay. *Constr Build Mater* 36:538–548
22. Knox EM, Cowling MJ (2000) Durability aspects of adhesively bonded thick adherend lap shear joints. *Int J Adhes Adhes* 20(4):323–331
23. Broughton W, Mera R (1999) Environmental degradation of adhesive joints, accelerated testing. NPL Rep CMMT A 197:1–25
24. Hewson NR (2003) Prestressed concrete bridges: design and construction. Thomas Telford, London
25. British Standards Institution (1999) BS EN 12615 Products and systems for the protection and repair of concrete structures. Test methods. Determination of slant shear strength. BSI, London
26. Momayez A, Ehsani MR, Ramezani pour AA, Rajaie H (2005) Comparison of methods for evaluating bond strength between concrete substrate and repair materials. *Cem Concr Res* 35(4):748–757
27. British Standards Institution (2009) BS EN 12390-6 Testing hardened concrete. Tensile splitting strength of test specimens. BSI, London
28. British Standards Institution (2009) BS EN 12390-5 Testing hardened concrete. Flexural strength of test specimens. BSI, London
29. British Standards Institution (2004) BS EN 12504-4 Testing concrete in structures. Determination of ultrasonic pulse velocity. BSI, London
30. Correlatedsolutions.com (2015) Correlated solutions. Accessed Feb 2015
31. British Standards Institution (2015) BS 8500-2 concrete—complementary british standard to BS EN 206. Part 2: specification for constituent materials and concrete. BSI, London
32. British Standards Institution (2013) BS 1881-125 Testing concrete. Methods for mixing and sampling fresh concrete in the laboratory. BSI, London
33. Comité Euro-International du Béton (2012) CEB-FIP. fib bulletin 55: model code 2010—final draft, vol 1. Lausanne, Switzerland
34. Jackson N, Dhir R (1997) Civil engineering materials, vol 4. Palgrave Macmillan, Basingstoke
35. Neville AM (2011) Properties of concrete, 5th edn. Pearson, Edinburgh